Application of a low-cost bagasse carbon-red mud (BCRM) adsorbent for adsorption of methylene blue cationic dye: adsorption performance, kinetics, isotherm, and thermodynamics

Yizhi Wang[a], Linye Zhang[a,*], Zhiwei Yan[a], Luhua Shao[a], Hong Kang[a], Guangtao Wei[b,*], Ming Zhou[a]

[a]School of Chemistry and Chemical Engineering, Guangxi University, Nanning 530004, China, email: yezi@gxu.edu.cn (L. Zhang)
[b]Guangxi Key Laboratory of Petrochemical Resource Processing and Process Intensification Technology, Nanning 530004, China, Tel./Fax: +86 771 323 3718; email: gtwei@hotmail.com

ABSTRACT

To understand adsorption property of bagasse carbon-red mud (BCRM), a low-cost adsorption material prepared from waste solid red mud and bagasse, for disposal of organic dyes in wastewater, the adsorption of methylene blue (MB) from aqueous solution on BCRM has been studied, and the adsorption treatment of real textile wastewater was also investigated. Characterization of BCRM was achieved by scanning electron microscope and nitrogen adsorption–desorption analysis. Effects of adsorption time, BCRM dosage, initial concentration, temperature, and initial pH on the adsorption of MB were explored. From the characterization of adsorbent, it can be seen that the prepared BCRM was a porous material composed of particles with rough surface and loose structure, and an excellent mesoporous material with high specific surface area and good mesopore structure. The adsorption results showed that the data fitted better with pseudo-second-order kinetic model ($R^2 = 0.9995$) than pseudo-second-order kinetic and intraparticle diffusion models. Langmuir model was better fit isotherm for MB adsorption on BCRM than Freundlich and Dubinin–Radushkevich adsorption isotherms. It can be drawn that MB adsorption on BCRM was a monolayer adsorption and the adsorption occurred at specific homogeneous sites on the adsorbent. The results of adsorption thermodynamics indicated MB adsorption on BCRM was a spontaneous, endothermic, and physical process. The adsorption treatment of real textile wastewater by BCRM implied BCRM was an effective and regenerable adsorbent for removal of dye from wastewater.

Keywords: Red mud; Bagasse; Adsorption; Kinetic; Isotherm; Thermodynamics; Textile wastewater

1. Introduction

Dyes normally have complex aromatic structures in molecules, providing dyes with thermal, physico-chemical and optical stability, and most of dyes belong to the refractory organic pollutants. Due to their color, dyes discharged into natural streams and rivers could decrease sunlight penetration into water and reduce the photosynthesis, which results in problem of water deterioration. Dye wastewater has brought damages to human beings, other individual

*Corresponding authors.

species, and natural biological communities due to the fact that dyes have certain toxicity, carcinogenic, and mutagenic properties [1]. Treatment of dye wastewater, i.e. disposal of organic dyes in water, is a significant research field in water treatment [2–4]. Conventional physicochemical and biological processes have been developed to remove dyes from aqueous solution for reducing their environmental impact on receiving water. The usual processes for disposal of dyes in wastewater are mainly photodegradation, coagulation and flocculation, chemical oxidation, membrane separation, reverse osmosis, and microbial biodegradation. However, there are still some limitations in the application of the above processes due to high cost, low removal efficiency, and secondary pollution. For low cost, high removal efficiency, and simple process, adsorption has been an attractive and alternative way for the disposal of dyes in wastewater [5–7]. In adsorption process of dye wastewater, a low cost and regenerable adsorbent with high adsorption capacity is crucial for the successful application of adsorption treatment.

Red mud (RM) is a waste residue during the extraction of alumina from bauxite. For one ton of alumina manufactured in Bayer process, 1–1.5 tons (dry weight) of RM residue are normally generated [8]. RM is strongly alkaline and toxic material because of high calcium and sodium oxides and hydroxides, which can cause great harm to environment. Bagasse is an important by-product of sugarcane milling process when producing sucrose-rich juice from sugarcane. Normally, two tons of bagasse are produced for one ton of sucrose. For many years, there has been an accumulation of bagasse due to the increase in sucrose production, and a considerable amount of bagasse was only burnt directly to heat water in boiler. Even though some heating energy is gained, the direct combustion of bagasse is not a highest-value way for bagasse reuse. Both aluminum and sucrose are pillar industries of Guangxi Zhuang Autonomous Region in China, so eco-economy treatments of RM and bagasse are very useful for economic development and environmental protection in Guangxi Zhuang Autonomous Region. Therefore, utilization of RM and bagasse to prepare adsorbent for adsorption of environmental pollutants in wastewater, especially for refractory organic pollutants, can not only dispose the waste material but also reduce cost of wastewater treatment in the process. Bagasse has been used as adsorbents for removal of various dyes from aqueous solution. Zhang et al. reported the adsorption of rhodamine B and basic blue 9 on milled sugarcane bagasse [9], and Mitter et al. analyzed the removal of acid alizarin violet N by using sugarcane bagasse as

adsorbent [10]. Amin prepared different activated carbons using bagasse pith as raw material, and then studied the removal of reactive orange dye from aqueous solutions by the activated carbons [11]. However, as in the above mentioned literatures, the regeneration and reuse of adsorbents, which were prepared from bagasse material and used in disposal of organic dyes in water, was not studied in most reports. In recent years, removal of various dyes from aqueous solution using raw or activated RM as adsorbents has also been reported in many published papers [12,13]. Wang et al. reported the adsorption of MB from aqueous solution by raw and activated RM, and both heat treatment and acid treatment by HNO_3 reduced the adsorption capacity of RM [14]. Çoruh et al. also studied the adsorption of MB from aqueous solution by raw and activated RM, and they found that heat treatment had almost no effects on the adsorption capacity of RM [15]. However, acid treatment of RM by HCl increased adsorption capacity of RM in Çoruh's study, and compared with 5.86 mg/g of raw RM, the capacity of acid-treated RM increased to 6.75 mg/g [14]. Even so, the adsorption capacities of activated RM were relatively low. Hence, preparation of an effective and regenerable adsorbent using RM as main materials might be useful for adsorption of dye pollutions from wastewater.

Bagasse carbon-red mud (BCRM), a low-cost adsorption material prepared from waste solid RM and bagasse, has been previously developed in our laboratory. To explore the applicability of adsorption treatment of dye wastewater by BCRM, the removal of dye from water and the treatment of real textile wastewater were studied in this paper. Methylene blue (MB), a typical cationic dye, is often founded in dye wastewater. Owing to its non biodegradation and stability, MB can exist stably in the dye wastewater. For the reasons above, MB was usually selected as a model compound to study the adsorption performance of dye on prepared adsorbents. Hence, to correctly understand the adsorption property of BCRM for removal of dye pollutions from water, MB was also selected as the model compound in this study.

2. Materials and methods

2.1. Materials and chemical reagents

RM in the study was obtained from an industrial Bayer's process in Guangxi Aluminum Corporation, in Guangxi Zhuang Autonomous Region, China. Prior to use, the RM was dried at 105°C and then ground to less than 0.15 mm. Bagasse was obtained from

Guangxi East Asia Sugar Group in Guangxi Zhuang Autonomous Region, China. The air-dried bagasse was also ground to less than 0.15 mm before using.

All chemicals and reagents used in the study, including NaOH, HNO₃, and MB, were of analytical reagent grade. The structure and characteristics of MB are presented in Table 1.

2.2. Preparation of BCRM adsorbent

Three gram of RM was mixed with bagasse under the mass ratio of 0.2:1, and then 10 mL of 1 mol/L HNO_3 was added with constant stirring. After about 20 min, the mixture was dried at 378 K and then calcined at 573 K for 1 h. When the calcination was finished, BCRM was obtained, and ground to less than 0.15 mm. The adsorption capability of prepared BCRM was evaluated by the removal efficiency of MB, which was obtained from the adsorption experiment.

2.3. Characterization of adsorbent

Scanning electron microscope (SEM) picture was obtained with an S-3400 N SEM (Hitachi, Japan). Surface area and pore volume of adsorbent, degassed under vacuum at 523 K for 18 h, were measured by N_2 adsorption–desorption isotherm at 77 K using an automatic adsorption apparatus (JW-BK1212W, JWGB, China).

2.4. Adsorption studies

Adsorption experiments were carried out in batch technique. MB solution with desired initial

Table 1
Properties of MB

Index	Methylene blue
Molecular structure	
Molecular formula	$C_{16}H_{18}ClN_3S$
Molecular weight	319.86
Hazard class	22-36/37/38-11
Hazard codes	X_n
Safety statements	26-36-24/25-16-7

concentration was obtained by dilution of MB stock solution (1,000 mg/L). Fifty milliliter of the MB solution was placed in 250 mL stoppered conical flask, and then adsorbent was added. The 250 mL stoppered conical flask was fixed in a thermostatic water bath oscillator and stirred at speed of 150 rpm. The pH of the solution was adjusted to desired value by addition of 1 mol/L HNO₃ or 1 mol/L NaOH solution. At the end of the adsorption, the adsorbent was separated from the solution by centrifugation at 3,500 rpm for 10 min. The concentration of MB in supernatant was determined at maximum absorbance wavelength of 665 nm using a visible spectrophotometer (VIS-722, SHYK, China), and then the removal percentage of MB (η) and the amount of MB adsorbed on adsorbent (q_t) were calculated, respectively.
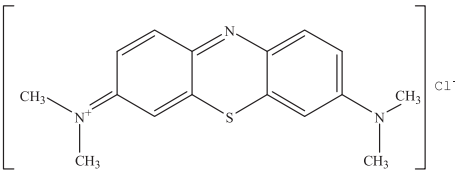
Adsorption treatment of textile wastewater was investigated with a real wastewater. The UV_{254} of wastewater, which reflects the amount of humic type of macromolecular organic matter and aromatic compounds in water, was analyzed at absorbance wavelength of 254 nm using a UV–Visible spectrophotometer (UV–Vis-752 N, SHYK, China), and the removal percentage of UV_{254} (η_{UV254}) was calculated. The color degree of wastewater before or after adsorption treatment was determined by dilution multiple method.

3. Results and discussion

3.1. Characterization of adsorbent

The SEM picture of BCRM is presented in Fig. 1(A). As showed in Fig. 1(A), BCRM was a porous material composed of particles with rough surface and loose structure, and the particle size of BCRM was in the range of 0.5–4 μm. The surface morphology of BCRM indicated that BCRM might be a good adsorbent for wastewater treatment. The N_2 adsorption–desorption isotherms and pore size distributions BCRM is presented in Fig. 1(B). The isotherms of BCRM exhibited type IV shape, corresponding to mesoporous adsorption [16]. Moreover, as seen from the BJH pore size distributions of BCRM (inset figures in Fig. 1(B)), the mesopore volume of BCRM occupied a considerable proportion in the sum volume of BCRM. The type IV isotherm and BJH pore size distribution of BCRM revealed that the prepared BCRM was one kind of mesoporous materials. Data of surface area and pore structure of RM and BCRM are presented in Table 2. Compared with 11.537 m²/g of RM, the multi point BET surface area of BCRM increased to 16.603 m²/g. And the mesopore volume percentage of BCRM reached
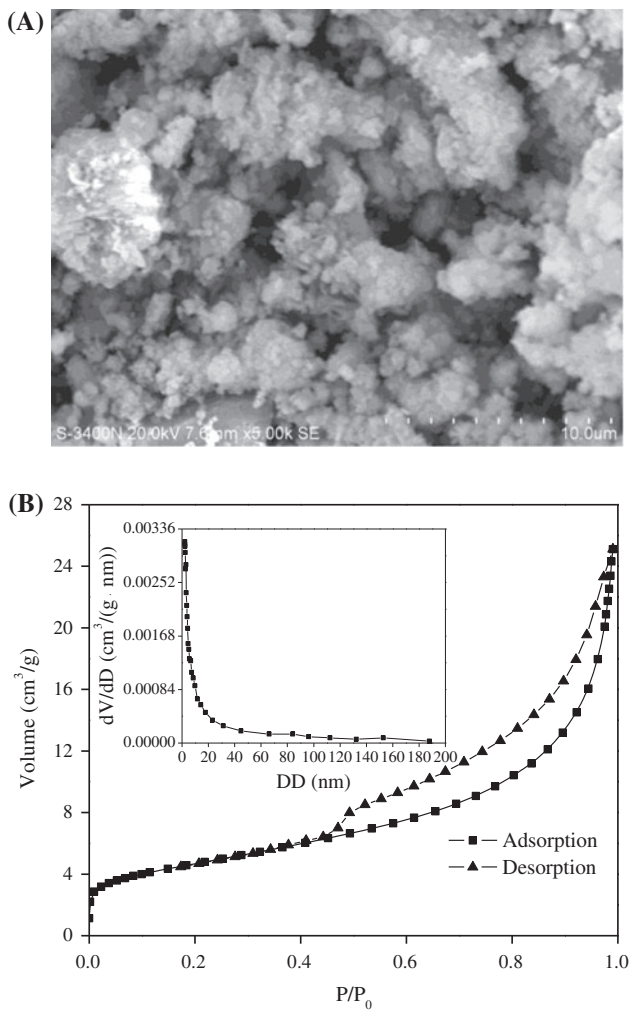
Fig. 1. (A) SEM picture of BCRM. (B) Adsorption–desorption isotherm and BJH pore size distribution of BCRM.

71.47%. From the characterization of adsorbent, it was concluded that the prepared BCRM was an excellent mesoporous material with high specific surface area and good mesopore structure.

3.2. Adsorption performance

3.2.1. Effect of adsorption time

The adsorption of MB onto BCRM was investigated by varying adsorption time from 5 to 240 min to conclude the adequate adsorption equilibrium time. As showed in Fig. 2, the removal of MB reached adsorption equilibrium at time of 120 min, and the removal efficiency of MB was 86.76%. It was found that the adsorption rate of MB rapidly increased in the first 5 min, and then changed slowly until the removal efficiency of MB reached a constant value. High concentration gradient of MB, available surface area, and vacant site of BCRM could be responsible for the rapid adsorption at the adsorption beginning. After the stage of rapid adsorption, MB concentration and available vacant site of BCRM decreased, which led to a sharp decrease of adsorption rate.
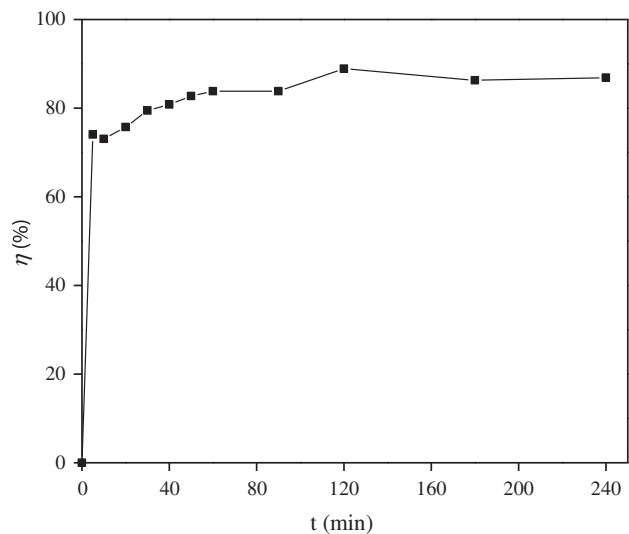

Fig. 2. Effect of adsorption time on MB adsorption (dosage = 6 g/L, C_0 = 30 mg/L, and initial pH of solution and room temperature).

Table 2
Data of surface area and pore structure of RM and BCRM

Adsorbent	Surface area (m^2/g)			Pore volume (cm^3/g)		Pore diameter (nm)			MVP (%)
	S_{mp}	S_{BJHa}	S_{BJHd}	v_{BJHa}	v_{BJHd}	$r_{average}$	r_{BJHa}	r_{BJHd}	
RM	11.537	10.105	11.099	0.031	0.032	10.945	12.283	11.359	53.68
BCRM	16.603	15.559	20.223	0.039	0.041	9.360	9.963	8.095	71.47

Note: Mp—multi point; BJHa—BJH adsorption; BJHd—BJH desorption; MVP (%)—mesopore volume percentage.

3.2.2 Effect of BCRM dosage

The effect of BCRM dosage on adsorption of MB was investigated. As shown in Fig. 3, the removal efficiency of MB increased from 54.67 to 96.35% with the dosage increase from 2 to 14 g/L, and the removal efficiency of MB revealed a fast increase until the dosage reached 6 g/L, which was ascribed to the increase of available adsorption site and surface area of BCRM adsorbent. As the dosage continued to increase from 6 to 14 g/L, the increase of removal efficiency changed slowly. For example, the removal efficiency of MB only reached 96.35% at dosage of 14 g/L, compared with 86.75% at dosage of 6 g/L.

3.2.3 Effects of initial MB concentration and temperature

The effect of initial MB concentration on adsorption of MB was investigated under different temperature. As shown in Fig. 4, the removal efficiency of MB decreased with the increase of initial concentration in the range of 10–100 mg/L. However, equilibrium adsorption capacity of BCRM (q_e) increased with increasing initial concentration. The increase of q_e was ascribed to the change of concentration gradient. The concentration gradient at higher initial concentration enhanced the probability of collision between MB molecules and BCRM. With the temperature increase from 298 to 323 K, the q_e increased from 9.64 to 10.60 mg/g, indicating that the adsorption of MB on the BCRM was endothermic in nature. The increase of
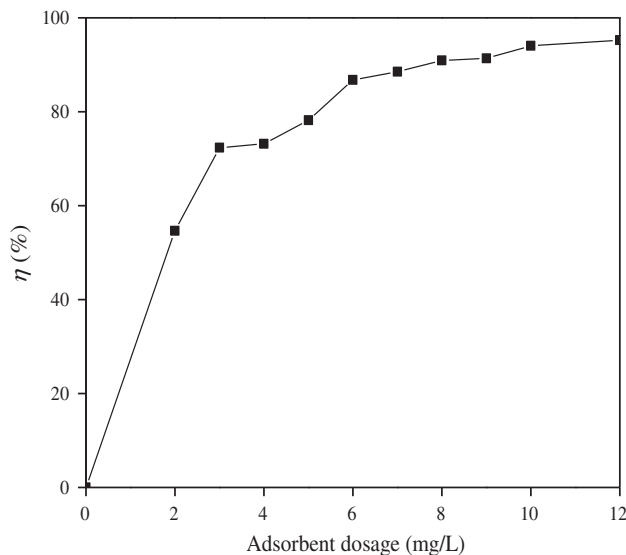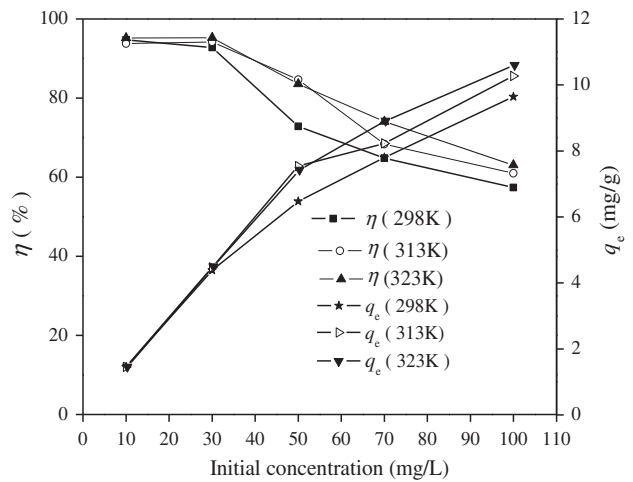

Fig. 4. Effect of initial concentration and temperature on MB adsorption ($t = 120$ min, dosage = 6 g/L, and initial pH of solution).

q_e with the temperature increase might be attributed to the increased mobility of MB in water and the high availability of active surface sites on BCRM at high temperature [17].

3.2.4 Effect of initial pH

The effect of initial pH of solution on adsorption of MB was investigated. As shown in Fig. 5, the removal efficiency of MB showed only a slight increase with the increase of pH from 2 to 12, indicating that the initial pH of solution only had a little effect on the MB
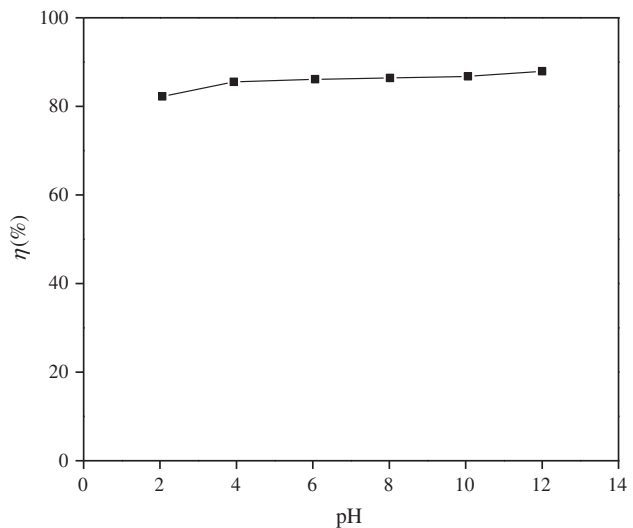

Fig. 3. Effect of BCRM dosage on MB adsorption ($t = 120$ min, $C_0 = 30$ mg/L, and initial pH of solution and room temperature).

Fig. 5. Effect of pH on MB adsorption ($t = 120$ min, $C_0 = 30$ mg/L, dosage = 6 g/L, and room temperature).

adsorption by BCRM adsorbent. The amount of negatively charged BCRM surface would increase with the increasing pH, so more electrostatic interactions between positive charge of MB and negatively charged BCRM surface could be the reason for the slight increase of removal efficiency with pH increasing. However, all the removal efficiencies in the pH 2–12 region reached a relatively high value, and the smallest removal efficiency appeared at pH 2 even reached 82.26%. Hence, the BCRM used as adsorbent in adsorption process had a wide applicable range of pH.

3.2.5. Maximum adsorption capacities of different adsorbents for MB

According to the reported references, preparation of modified RM adsorbent from RM waste is mainly via the method of acid activation or heat activation. The maximum adsorption capacities of raw RM and modified RM for MB were provided in some literatures. The maximum adsorption capacities of raw RM and HNO_3-activated RM reported by Wang were 2.49 and 1.02 mg/g, respectively [14]. The maximum adsorption capacities of raw RM, HCl-activated RM and heat-activated RM reported by Çoruh were 5.86, 6.75, and 3.28 mg/g, respectively [15]. However, the maximum adsorption capacity of raw RM and BCRM for MB in our present work reached 0.51 and 10.05 mg/g, respectively. Compared with that of other modified RM adsorbents above, the maximum adsorption capacity of BCRM was the highest. A conclusion could be safely drawn that BCRM adsorbent had a high adsorption capacity for adsorption of organic pollution from wastewater.

3.3. Adsorption kinetics

For interpreting the controlling theory of MB adsorption process on BCRM, kinetic experimental data were analyzed and modeled by using three kinetic equations, i.e. pseudo-first-order kinetic equation, pseudo-second-order kinetic equation, and intraparticle diffusion kinetic equation.

Pseudo-first-order kinetic equation can be expressed as Eq. (1) [18]:

$$\ln(q_e - q_t) = \ln q_e - k_1 t \tag{1}$$

where q_t is the amount of MB adsorbed (mg/g) at time t, q_e is the amount of MB adsorbed (mg/g) at equilibrium, and k_1 is the rate constant of pseudo-first-order adsorption (L/min). The plot of $\ln(q_e - q_t)$ vs. t is shown in Fig. 6(A). The value of calculated q_e
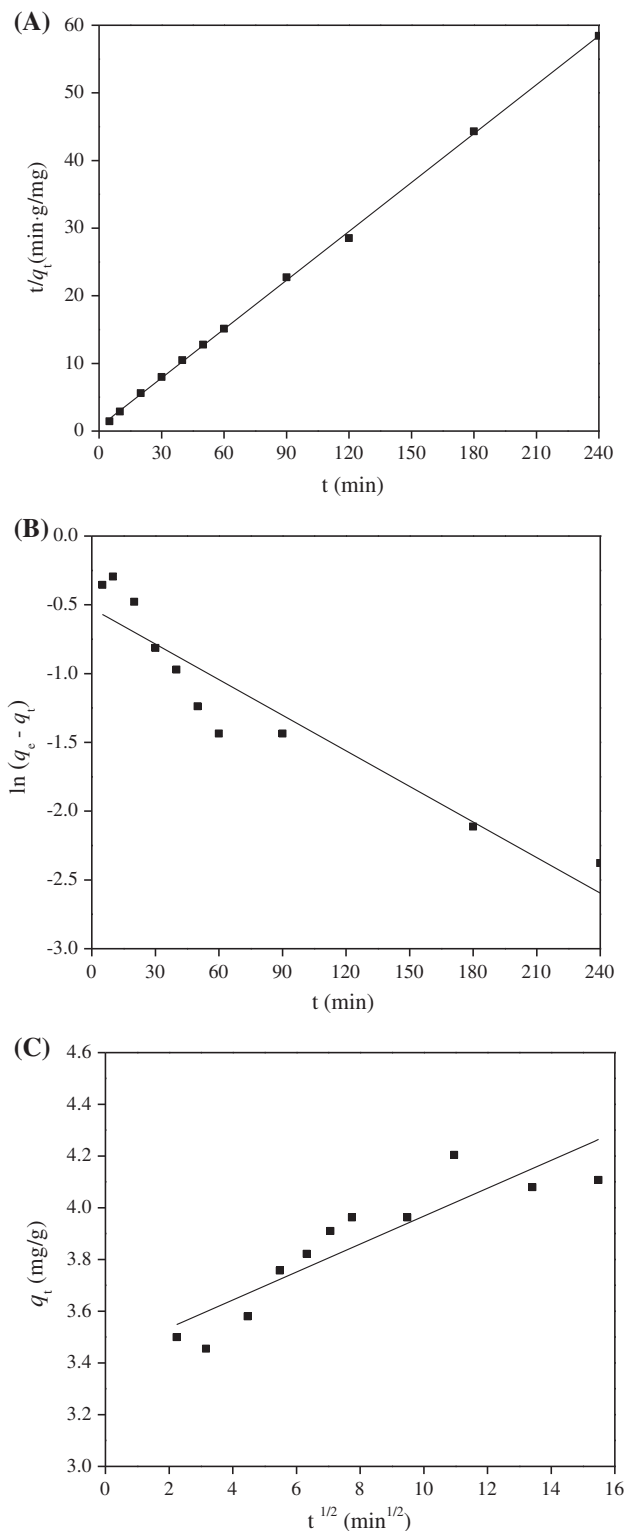

Fig. 6. (A) Plot of pseudo-first-order kinetic equation kinetic equation for MB adsorption on BCRM. (B) Plot of pseudo-second-order kinetic equation for MB adsorption on BCRM. (C) Plot of intraparticle diffusion equation for MB adsorption on BCRM.

and the square of correlation coefficient (R^2) are presented in Table 3. Because R^2 was 0.8753 and the calculational q_e was obviously less than the experimental q_e, pseudo-first-order equation was not adequate for depicting the adsorption behavior of MB on BCRM for the entire adsorption period.

Pseudo-second-order equation can be expressed as Eq. (2) [19]:

$$\frac{t}{q_t} = \frac{1}{k_2 q_e^2} + \frac{t}{q_e} \tag{2}$$

where k_2 is the rate constant of pseudo-second-order adsorption (g/(mg min)). The plot of t/q_t vs. t was straight line as shown in Fig. 6(B). The value of k_2, q_e, and R^2 are given in Table 3. The R^2 of pseudo-second-order equation was 0.9995, indicating the good applicability of pseudo-second-order equation used for fitting MB adsorption by BCRM. Pseudo-second-order model, containing all the rate controlling process of adsorption such as external film diffusion, surface adsorption, intraparticle diffusion, and so on [20], could truly reflect the mechanism of the MB adsorption process on BCRM.

Intraparticle diffusion equation can be expressed as Eq. (3) [21]:

$$q_t = k_d t^{1/2} + C \tag{3}$$

where k_d and C are the intraparticle diffusion rate constant (mg/(g min$^{1/2}$)) and the constant correlation with the thickness of boundary layer, respectively. The plot of q_t vs. $t^{1/2}$ is shown in Fig. 6(C). The plot of intraparticle diffusion kinetics, which was drawn

using experimental data in the present study, did not pass through the origin, demonstrating that intraparticle diffusion was not the only rate controlling process for MB adsorption on BCRM [22]. The deviation of the plot from the origin was ascribed to the difference in the rate of mass transfer in the initial and final stages of the adsorption [23]. Furthermore, base on calculation from slope and intercept of the plot, the value of k_d, C, and R^2 are listed in Table 3. In short, the adsorption of MB on BCRM was rather complex and involved more than one diffusive resistance.

3.4. Adsorption isotherm

In order to explore relationship between the amount of adsorbed MB and the concentration of MB under different temperature, Langmuir, Freundlich, and Dubinin–Radushkevich adsorption isotherms were selected to analyze the adsorption isotherm.

Langmuir adsorption isotherm is the model applied to describe monolayer adsorption and adsorption usually occurs at specific homogeneous sites on the adsorbent [24]. The Langmuir equation is shown as Eq. (4):

$$q_e = \frac{q_m b C_e}{1 + b C_e} \tag{4}$$

where q_m is the greatest equilibrium adsorption capacity (mg/g) and b is the adsorption equilibrium constant (L/mg). The linearized form of Langmuir equation is given by Eq. (5) and the values of q_m and b can be calculated from the plot of C_e/q_e against C_e.

$$\frac{C_e}{q_e} = \frac{1}{q_m b} + \frac{C_e}{q_m} \tag{5}$$

A dimensionless constant separation factor indicating the essence of Langmuir model is given by Eq. (6):

$$R_L = \frac{1}{1 + b C_0} \tag{6}$$

Favorable adsorption occurs, when the R_L ranges from 0 to 1. If $R_L = 0$ adsorption is irreversible; if $R_L = 1$ adsorption is linear. Unfavorable adsorption is established, when the value of R_L is greater than 1.

Freundlich adsorption isotherm is empirical model based on heterogeneous surface and is expressed as Eq. (7) [25]:

$$q_e = K_F C_e^{1/n} \tag{7}$$

Table 3
Kinetic constants for adsorption of MB on BCRM[a]

Kinetic constant	BCRM
Pseudo-first-order equation	
q_e (mg/g)	0.59
K_1	0.5266
R^2	0.8753
Pseudo-second-order equation	
K_2	0.1137
q_e (mg/g)	4.14
R^2	0.9995
Intraparticle diffusion equation	
k_d	0.054
C	3.4273
R^2	0.7844

[a]Experimental q_e is 4.20 mg/g.

where K_F and n are Freundlich adsorption isotherm constants. The linearized form of Freundlich equation is given by Eq. (8) and the values of K_F and n can be calculated from the plot of $\ln q_e$ against $\ln C_e$.

$$\ln q_e = \ln K_F + \frac{1}{n} \ln C_e \qquad (8)$$

Dubinin–Radushkevich adsorption isotherm is usually employed to estimate the porosity apparent free energy and the characteristic of adsorption [26,27], due to its assumption of heterogeneous surface or unconstant sorption potential. The equation and the linearized form of Dubinin–Radushkevich adsorption isotherm are given as follows:

$$q_e = q_m \exp(-K_{DR}\varepsilon^2) \qquad (9)$$

$$\ln q_e = \ln q_m - K_{DR}\varepsilon^2 \qquad (10)$$

where K_{DR} is the activity coefficient related to adsorption energy, ε is the Polanyi potential, and ε can be calculated from Eq. (12):

$$\varepsilon = RT \ln(1 + 1/C_e) \qquad (11)$$

where R is the gas constant (kJ/(mol K)), T is the temperature (K). The values of K_{DR} and q_m can be calculated from the plot of $\ln q_e$ against ε^2. The mean free energy (E) is free energy change when adsorbates transfer from the solution to solid surface, and E can be calculated from Eq. (13):

$$E = \frac{1}{\sqrt{2K_{DR}}} \qquad (12)$$

The plots of Langmuir, Freundlich, and Dubinin–Radushkevich adsorption isotherms for the MB adsorption on BCRM at different temperature are shown in Fig. 7. The isotherm parameters from all the models and the correlation coefficients calculated from all linear regression (as shown in Fig. 7) are listed in Table 4. According to the correlation coefficient values of isotherm, it was observed that, compared with Freundlich adsorption equation and Dubinin–Radushkevich adsorption equation, Langmuir adsorption equation had a perfect fit for the equilibrium data under different temperature. It was concluded that the behavior of MB adsorption process on BCRM was monolayer adsorption and adsorption occurred at specific homogeneous sites on the adsorbent. The calculated values of R_L for Langmuir model were in the
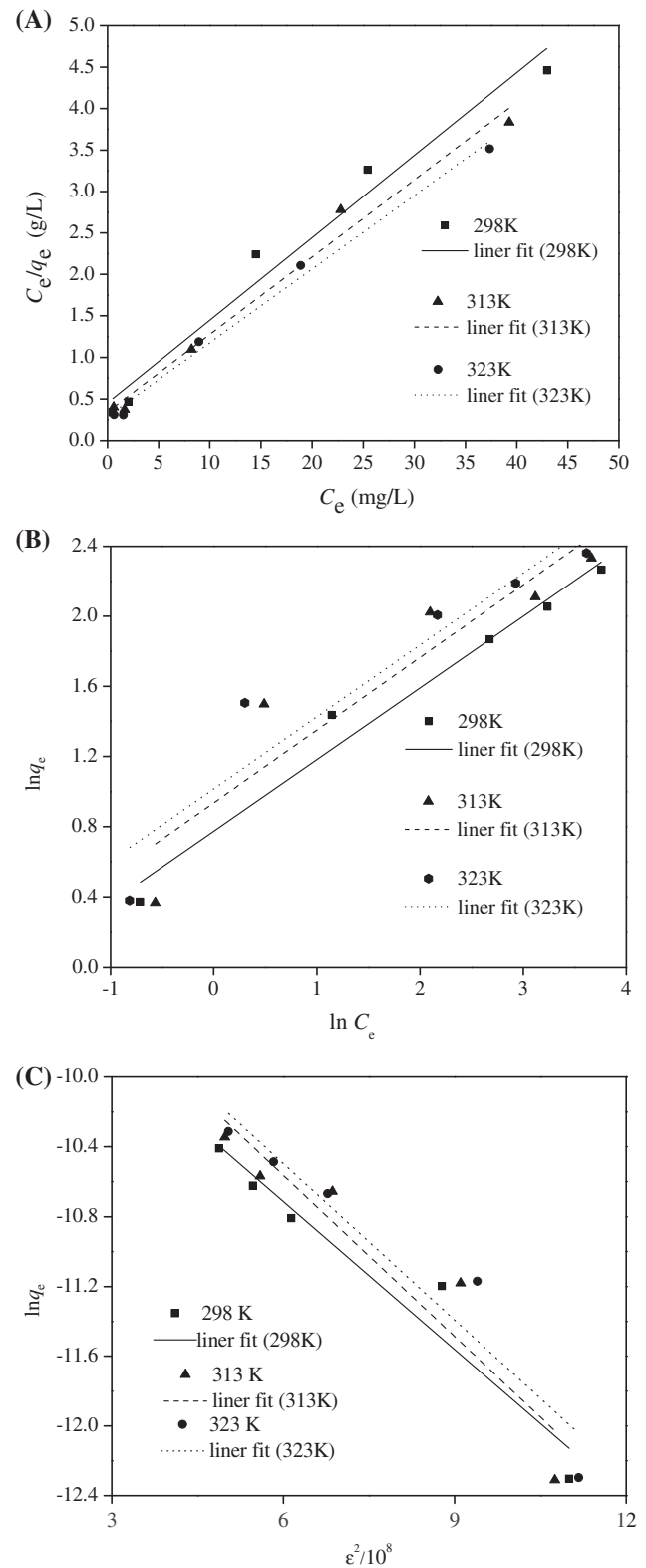

Fig. 7. (A) Plots of Langmuir isotherm model for MB adsorption on BCRM. (B) Plots of Freundlich isotherm model for MB adsorption on BCRM. (C) Plots of Dubinin–Radushkevich isotherm model for MB adsorption on BCRM.

Table 4
Isotherm parameters for MB adsorption on BCRM

Isotherm parameters	Temperature		
	298 K	313 K	323 K
Langmuir isotherm			
b (L/mg)	0.22	0.27	0.70
q_m (mg/g)	10.05	10.73	11.27
R_L	0.04–0.31	0.04–0.27	0.01–0.13
R^2	0.9651	0.9803	0.9902
Freundlich isotherm			
K_F	2.37	2.53	2.76
n	2.60	2.41	2.44
R^2	0.9009	0.8302	0.8671
Dubinin–Radushkevich isotherm			
$K_{DR} \times 10^{-9}$	2.83	3.08	2.99
$q_m \times 10^{-4}$ (mol/g)	1.21	1.63	1.67
E (kJ/mol)	1.33	1.27	1.29
R^2	0.9242	0.8651	0.8970

range of 0.04–0.31 at 298 K, 0.04–0.27 at 313 K and 0.01–0.13 at 323 K, respectively, indicating the adsorption of MB on BCRM was a favorable process.

3.5. Adsorption thermodynamics

Adsorption thermodynamic parameters including free energy change ΔG, entropy change ΔS, and enthalpy change ΔH were obtained from the following equations:

$$K_a = \frac{q_e}{C_e} \tag{13}$$

$$\Delta G = -RT \ln K_a \tag{14}$$

$$\ln K_a = \frac{\Delta S}{R} - \frac{\Delta H}{RT} \tag{15}$$

where K_a is the equilibrium constant. The thermodynamic parameters of MB adsorption onto BCRM are presented in Table 5. The negative values of ΔG suggested the feasibility and spontaneous nature of MB

adsorption on BCRM. The positive value of ΔH indicated the endothermic nature of MB adsorption process. The value of ΔS revealed the increased randomness in system when the adsorption process by BCRM was finished [17].

Low activation energies (5–40 kJ/mol) are characteristic of physical adsorption, while higher ones (40–800 kJ/mol) suggest chemisorption [28]. The activation energy (E_a) can be calculated from experimental data using a modified Arrhenius type equation related to surface coverage as follows:

$$S^* = (1 - \theta)e^{-E_a/RT} \tag{16}$$

$$\theta = 1 - \frac{C_e}{C_0} \tag{17}$$

where S^* is the sticking probability, θ is the surface coverage. The calculated E_a is also presented in Table 5. The E_a of MB adsorption on BCRM was 13.21 kJ/mol, which confirmed that the MB adsorption by BCRM was a physical adsorption.

3.6. Application and regeneration of BCRM for treatment of real textile wastewater

To verify the potential application and regeneration of BCRM in industry, adsorption treatment of a real textile wastewater was carried out under the adsorption condition of BCRM dosage 10 g/L, room temperature, adsorption time 120 min, and initial pH of wastewater (around 9). UV$_{254}$ of the raw wastewater was 3.50, and color degree was about 2000. The adsorption and regeneration for BCRM was recycled 4 times. When adsorption was finished in each recycle, the BCRM was separated by certification, and then was dried at 378 K. The dried BCRM was calcined in air at 573 K for 1 h and reused in adsorption experiment. The changes of removal percentage of UV$_{254}$ and color degree of wastewater with the recycle times of regenerated BCRM are shown in Fig. 8. As shown in Fig. 8, the removal percentage of UV$_{254}$ by fresh BCRM adsorbent reached 43.01%, and the color degree

Table 5
Thermodynamic parameters for MB adsorption process on BCRM

ΔG (kJ/mol)					
298 K	313 K	323 K	ΔH (kJ/mol)	ΔS (J/mol k)	E_a (kJ/mol)
−1.88	−2.60	−3.23	14.03	53.30	13.21

of treated wastewater decreased to 400. However, as seen from Fig. 8, the removal efficiency of UV_{254} and color degree of wastewater by the generated BCRM all reached almost the same values as those by the fresh BCRM. The used BCRM could be easily regenerated, and the adsorption capability of used BCRM was successfully recovered to the level of fresh BCRM via simple calcination in air at 573 K for 1 h. The results indicated that BCRM was an effective and regenerable adsorption material, and could be applicable for adsorption treatment of dye wastewater.

4. Conclusions

Low-cost BCRM adsorbent was an excellent mesoporous material with high specific surface area and good mesopore structure, and had a high adsorption capacity for adsorption of organic pollution from wastewater. The adsorption of MB cationic dye on BCRM was mainly affected by adsorption time, BCRM dosage, and initial MB concentration. It was found that, compared with traditional activated RM adsorbent, BCRM had a higher maximum adsorption capacity. Kinetic data of MB adsorption on BCRM fitted well with pseudo-second-order kinetic model. Adsorption data obeyed Langmuir adsorption isotherm very well, indicating that the behavior of MB adsorption process on BCRM was monolayer adsorption and adsorption occurred at specific homogeneous sites on the adsorbent. The positive value of ΔH indicated the endothermic nature of adsorption, and the negative value of ΔG showed the feasibility, and spontaneity of MB adsorption on BCRM. The value of E_a indicated MB adsorption on BCRM was a physical adsorption. Moreover, the results of adsorption treatment of a real textile wastewater showed that BCRM was effective in reducing the U_{254} and color degree of wastewater, and the used BCRM could be regenerated via simple calcination at 573 K in air. Hence, BCRM has good potential for use as an adsorbent to treat dye wastewater.
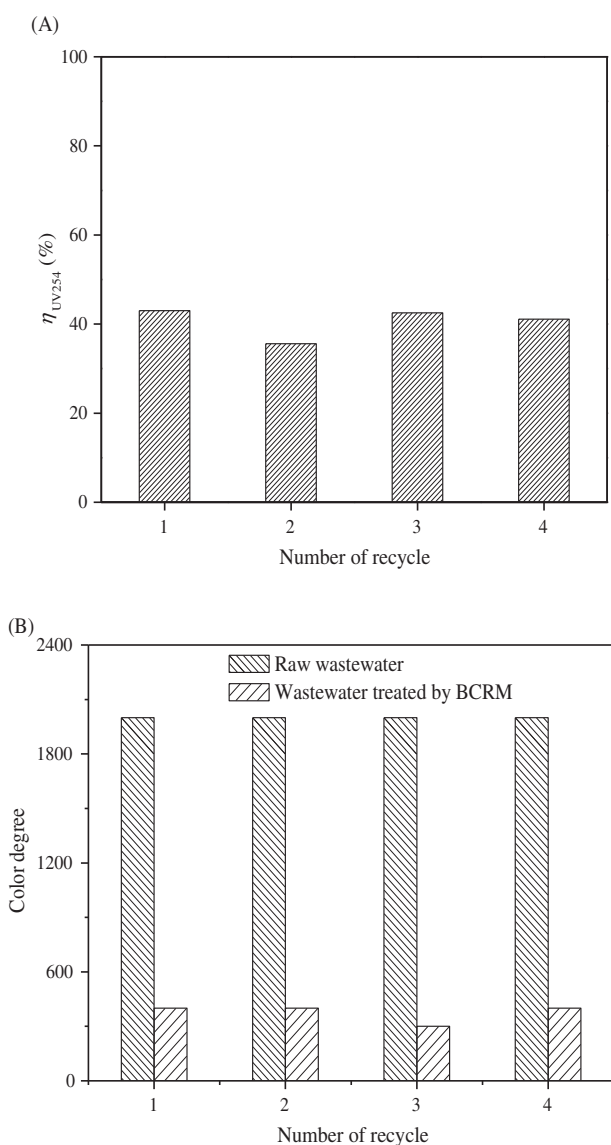
Fig. 8. (A) Change of removal percentage of UV_{254} with recycle times of generated BCRM. (B) Change of color degree of wastewater with recycle times of generated BCRM.

References

[1] P.S. Kumar, S. Ramalingam, C. Senthamarai, M. Niranjanaa, P. Vijayalakshmi, S. Sivanesan, Adsorption of dye from aqueous solution by cashew nut shell: Studies on equilibrium isotherm, kinetics and thermodynamics of interactions, Desalination 261 (2010) 52–60.
[2] R. Jain, P. Sharma, S. Sikarwar, J. Mittal, D. Pathak, Adsorption kinetics and thermodynamics of hazardous dye Tropaeoline 000 unto Aeroxide Alu C (Nano alumina): A non-carbon adsorbent, Desalin. Water Treat. 52 (2014) 7776–7783.
[3] A. Mittal, Removal of the dye, amaranth from waste water using hen feathers as potential adsorbent, Electron. J. Environ. Agric. Food Chem. 5 (2006) 1296–1305.

[4] J. Mittal, V. Thakur, A. Mittal, Batch removal of hazardous azo dye Bismark Brown R using waste material hen feather, Ecol. Eng. 60 (2013) 249–253.

[5] G. Sharmaa, M. Naushad, D. Pathania, A. Mittal, G.E. El-desoky, Modification of *Hibiscus cannabinus* fiber by graft copolymerization: Application for dye removal, Desalin. Water Treat. doi:10.1080/19443994.2014.904822.

[6] A. Mittal, V. Thakur, J. Mittal, H. Vardhan, Process development for the removal of hazardous anionic azo dye Congo red from wastewater by using hen feather as potential adsorbent, Desalin. Water Treat. 52 (2014) 227–237.

[7] J. Mittal, D. Jhare, H. Vardhan, A. Mittal, Utilization of bottom ash as a low-cost sorbent for the removal and recovery of a toxic halogen containing dye eosin yellow, Desalin. Water Treat. 52 (2014) 4508–4519.

[8] G. Lopes, L.R.G. Guilherme, E.S.T. Costa, N. Curi, H.G.V. Penha, Increasing arsenic sorption on red mud by phosphogypsum addition, J. Hazard. Mater. 262 (2013) 1196–1203.

[9] Z.Y. Zhang, I.M. O'Hara, G.A. Kent, W.O.S. Doherty, Comparative study on adsorption of two cationic dyes by milled sugarcane bagasse, Ind. Crops Prod. 42 (2013) 41–49.

[10] E.K. Mitter, G.C. dos Santos, É.J.R. de Almeida, L.G. Morão, H.D.P. Rodrigues, C.R. Corso, Analysis of acid alizarin violet N dye removal using sugarcane bagasse as adsorbent, Water Air Soil Pollut. 223 (2012) 765–770.

[11] N.K. Amin, Removal of reactive dye from aqueous solutions by adsorption onto activated carbons prepared from sugarcane bagasse pith, Desalination 223 (2008) 152–161.

[12] M. Shirzad-Siboni, S.J. Jafari, O. Giahi, I. Kim, L. Seung-Mok, Y. Jae-Kyu, Removal of acid blue 113 and reactive black 5 dye from aqueous solutions by activated red mud, J. Ind. Eng. Chem. 20 (2014) 1432–1437.

[13] A. Bhatnagar, V.J.P. Vilar, C.M.S. Botelho, R.A.R. Boaventura, A review of the use of red mud as adsorbent for the removal of toxic pollutants from water and wastewater, Environ. Technol. 32 (2011) 231–249.

[14] S.B. Wang, Y. Boyjoo, A. Choueib, Z.H. Zhu, Removal of dyes from aqueous solution using fly ash and red mud, Water. Res. 39 (2005) 29–138.

[15] S. Çoruh, F. Geyikçi, O.N. Ergun, Adsorption of basic dye from wastewater using raw and activated red mud, Environ. Technol. 32 (2011) 1183–1193.

[16] K.W. Sing, Reporting physisorption data for gas/solid systems with special reference to the determination of surface area and porosity, Pure Appl. Chem. 54 (1982) 2201–2218.

[17] G. Moussavi, R. Khosravi, The removal of cationic dyes from aqueous solutions by adsorption onto pistachio hull waste, Chem. Eng. Res. Des. 89 (2011) 2182–2189.

[18] L.Y. Zhang, H.Y. Zhang, Y.L. Tian, Z.S. Chen, L. Han, Adsorption of methylene blue from aqueous solutions onto sintering process red mud, Desalin. Water Treat. 47 (2012) 31–41.

[19] H. Daraei, A. Mittal, M. Noorisepehr, F. Daraei, Kinetic and equilibrium studies of adsorptive removal of phenol onto eggshell waste, Environ. Sci. Pollut. Res. 20 (2013) 4603–4611.

[20] A. Khaled, A.E. Nemr, A. El-Sikaily, O. Abdelwahab, Removal of direct N blue-106 from artificial textile dye effluent using activated carbon from orange peel: Adsorption isotherm and kinetic studies, J. Hazard. Mater. 165 (2009) 100–110.

[21] A.Y. Dursun, O. Tepe, G. Uslu, G. Dursun, Y. Saatci, Kinetics of Remazol Black B adsorption onto carbon prepared from sugar beet pulp, Environ. Sci. Pollut. Res. 20 (2013) 2472–2483.

[22] C.K. Lim, H.H. Bay, C.H. Neoh, A. Aris, Z.A. Majid, Z. Ibrahim, Application of zeolite-activated carbon macrocomposite for the adsorption of Acid Orange 7: Isotherm, kinetic and thermodynamic studies, Environ. Sci. Pollut. Res. 20 (2013) 7243–7255.

[23] W.H. Cheung, Y.S. Szeto, G. McKay, Intra-particle diffusion processes during acid dye adsorption onto chitosan, Bioresour. Technol. 98 (2007) 2897–2904.

[24] K.K. Pandey, G. Prasad, V.N. Singh, Mixed adsorbent for Cu(II) removal from aqueous solutions, Environ. Technol. Lett. 50 (1986) 547–554.

[25] A. Tabak, N. Baltas, B. Afsin, M. Emirik, B. Caglarc, E. Erend, Adsorption of Reactive Red 120 from aqueous solutions by cetylpyridinium-bentonite, J. Chem. Technol. Biotechnol. 85 (2010) 1199–1207.

[26] H. Daraeia, A. Mittal, M. Noorisepehr, J. Mittal, Separation of chromium from water samples using eggshell powder as a low-cost sorbent: Kinetic and thermodynamic studies, Desalin. Water Treat. 53 (2015) 214–220.

[27] A. Mittal, V. Thakur, V. Gajbe, Adsorptive removal of toxic azo dye Amido Black 10B by hen feather, Environ. Sci. Pollut. Res. 20 (2013) 260–269.

[28] D.M. Chen, J. Chen, X.L. Luan, H.P. Ji, Z.G. Xia, Characterization of anion–cationic surfactants modified montmorillonite and its application for the removal of methyl orange, Chem. Eng. J. 171 (2011) 1150–1158.